*in "Integrated Thin Films and Applications" edited by R.K. Pandey, P. Morris-Hotsenpiller, A. Roshko, U. Varshney, and D.E. Witter (Ceram. Trans. **86**, Westerville, OH, 1998) 233-43.*

THE MORPHOLOGY OF RUTILE (100), (101), AND (001) SURFACES: SINGLE CRYSTALS, HOMOEPITAXIAL FILMS, AND HETEROEPITAXIAL FILMS

Jennifer Giocondi, Jennifer B. Lowekamp, Gregory S. Rohrer, and Patricia A. Morris Hotsenpiller*
Department of Materials Science and Engineering
Carnegie Mellon University, Pittsburgh, Pennsylvania 15213-3890
*DuPont Company, Experimental Station, Wilmington, DE 19880-0356

ABSTRACT

Atomic force microscopy has been used to examine the structure of heteroepitaxial, homoepitaxial, and single crystal rutile surfaces with (100), (101), and (001) orientations. The single crystal surfaces were prepared by polishing and annealing. The homo- and heteroepitaxial films were grown by ion-beam sputter deposition on as-received rutile and sapphire substrates, respectively. In each case, the film thickness, growth rate, and growth temperature were held constant. Both classes of thin films have island-like surface morphologies that resulted from three dimensional growth. Island formation and sustained three dimensional growth during homoepitaxy is attributed to the relatively high impurity concentration in the rutile substrates and the anisotropy of rutile's surface energy. The surface morphologies of the heteroepitaxial films illustrate the combined influence of surface energy anisotropy and mismatch strain from the substrate/film interface.

INTRODUCTION

Crystalline TiO_2 films can potentially be used as photocatalysts for atmospheric pollution control, wastewater treatment, and solar energy conversion, as well as gas sensors, waveguides, and as components in a variety of electronic

devices. For many of these applications, surface morphology is an important structural characteristic. In this paper, we describe a set of experiments that were designed to explore the mechanisms of TiO_2 film growth and surface morphology development. Specifically, we have studied three cases where the morphologies of surfaces with the same orientation develop under different influences. First, we consider the morphologies of annealed single crystal rutile surfaces with the (100), (101), and (001) orientations. We assume that these surfaces represent a near equilibrium condition. Second, the morphologies of homoepitaxial rutile films with the same orientations are studied. In this case, the surface morphology is influenced by the quality of the substrate and rutile's anisotropic surface energies and growth rates. In the third and final case, we consider the surface morphology of heteroepitaxial rutile films that have the same orientations. In addition to the factors that influenced the growth of the homoepitaxial layers, the affect of mismatch strain at the film/substrate interface is illustrated.

EXPERIMENTAL

Polished single crystal rutile substrates were obtained from Commercial Crystal Laboratories, Naples, FL. The crystals were annealed in air to create a near equilibrium surface structure. During this treatment, the furnace was heated at a rate of 5 °C/min, held at 1000 °C for 1 h, and then cooled at 5 °C/min. This heat treatment was selected based on our observation that polished titania ceramics consisting of randomly oriented polycrystals form large surface facets during such a treatment.

The rutile films were grown by ion-beam sputter deposition (IBSD). This procedure, outlined below, is described in more detail in references [1,2]. Prior to growth, the chamber is evacuated to $1x10^{-7}$ torr. The growth atmosphere contained $1x10^{-4}$ torr Xe and $1x10^{-4}$ torr O_2. Deposition resulted from reactively sputtering a high-purity (99.995 %) Ti target with a Xe ion-beam from a 3 cm Kaufmann-type ion source. To isolate the effects of the substrate on film morphology, all of the films described here were 2000 Å thick and grown at a rate of 3 Å/min while maintaining a substrate temperature of 725 °C.

As-received, polished substrates were rinsed in high-purity methanol before being introduced to the vacuum chamber through a load-lock. Rutile crystals with (100), (101), and (001) orientations were used for homoepitaxial growth of rutile films of the same orientation and sapphire (0001), $(11\bar{2}0)$, and $(10\bar{1}0)$ substrates were used to grow heteroepitaxial films of (100), (101), and (001) oriented rutile, respectively. Rutherford backscattering spectrometry of 2 MeV $^4He^+$ ions was used to measure the thickness of the films and to check that they had the correct Ti to oxygen stoichiometry. X-ray diffraction was used to demonstrate that the films had a high degree of crystallinity; these results were described in more detail in two earlier publications [1,2].

The surface morphology of each sample was examined by ambient atmosphere atomic force microscopy (AFM) using a Park Scientific Instruments Scanning Probe Microscope. The microscope was operated in the contact mode using high aspect ratio Si ultralevers and constant forces in the 0.1 to 5 nN range. The images presented here are representative of many observations, with at least two different probe tips. The relationship between the surface features and the crystallographic axes of each sample were determined from backscattered Laue photographs.

EXPERIMENTAL RESULTS

The (100) and (101) single crystal surfaces had stepped morphologies consisting of several hundred nm wide terraces separated by small steps (See Fig. 1). On the (100) surface, the steps are 4 to 6 Å high, comparable to the magnitude of the lattice parameter (4.59 Å) in the [100] direction. On the (101) surface, the steps are small integer multiples of the approximately 2.5 Å spacing between adjacent (101) planes. For both the (100) and (101) surfaces, the directions of the steps varied from area to area, presumably due to small local deviations from the ideal orientation. However, the steps were always composed of straight segments meeting at corners, suggesting preference for certain low index orientations. For example, in Fig. 1b, the steps are aligned along [010] and $[\bar{1}01]$ directions.

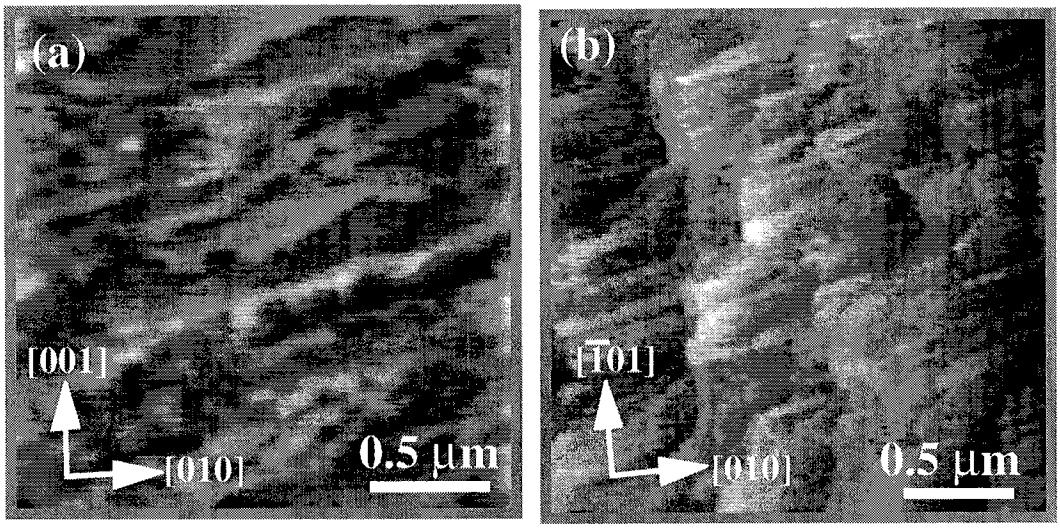

Figure 1. Topographic AFM images (a) the (001) rutile surface (b) the (101) rutile surface. In each image, the vertical black-to-white contrast is approximately 10 Å.

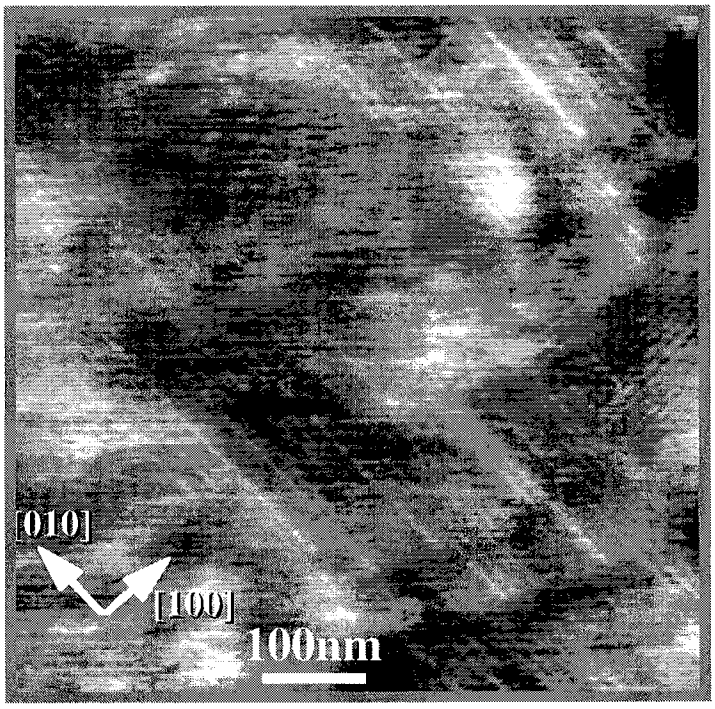

Figure 2. Topographic AFM images of the (001) rutile surface. The vertical black-to-white contrast is approximately 10 Å.

The structure of the (001) surface was distinct from the other two. It consisted of a cross hatch pattern of step features oriented along the [100] and [010] directions of the surface. Within domains, the steps exhibit a nearly periodic structure and are separated by about 10 nm. Because the vertical topography (2 Å) and spacing of these features are so small, they could only be partially resolved in any single image. The poorly resolved regions in Fig. 2 are probably due to surface contamination that is unavoidable during ambient AFM experiments.

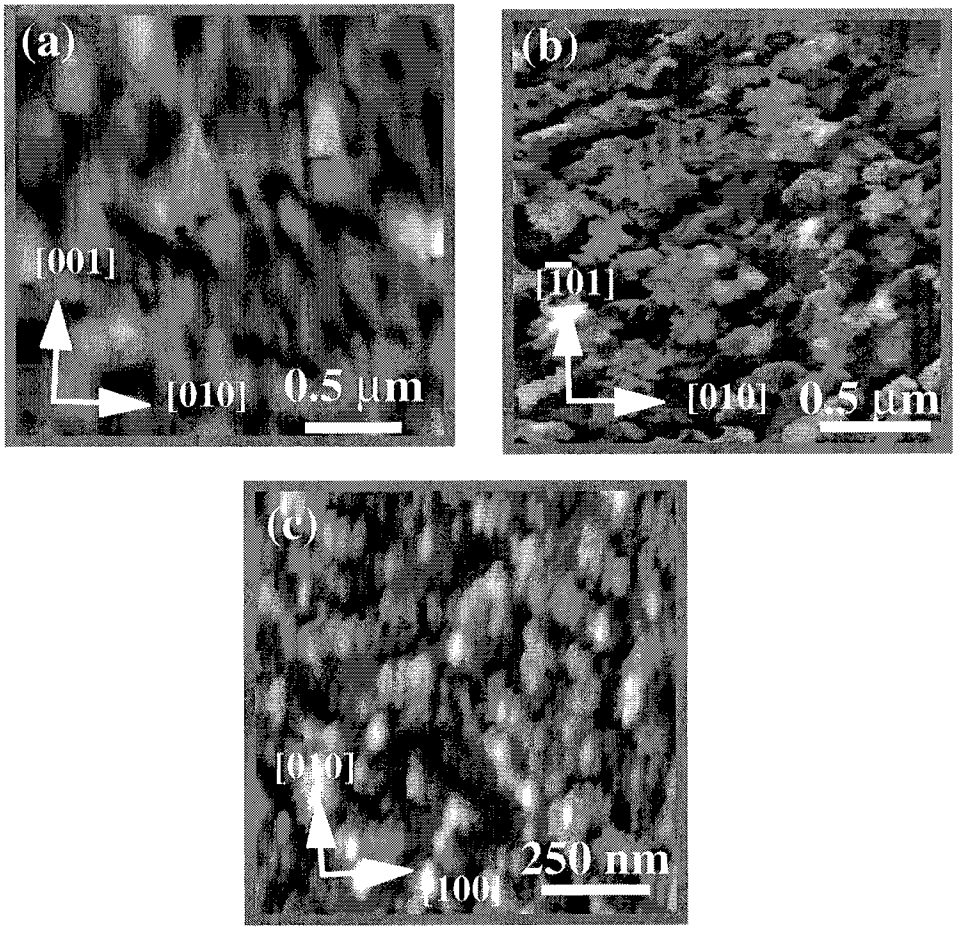

Figure 3. Topographic AFM images of homoepitaxial rutile films. (a) The (100) surface, the vertical black-to-white scale is 50 Å. (b) The (101) surface, the vertical scale is 150 Å. (c) The (001) surface, the vertical scale is 25 Å.

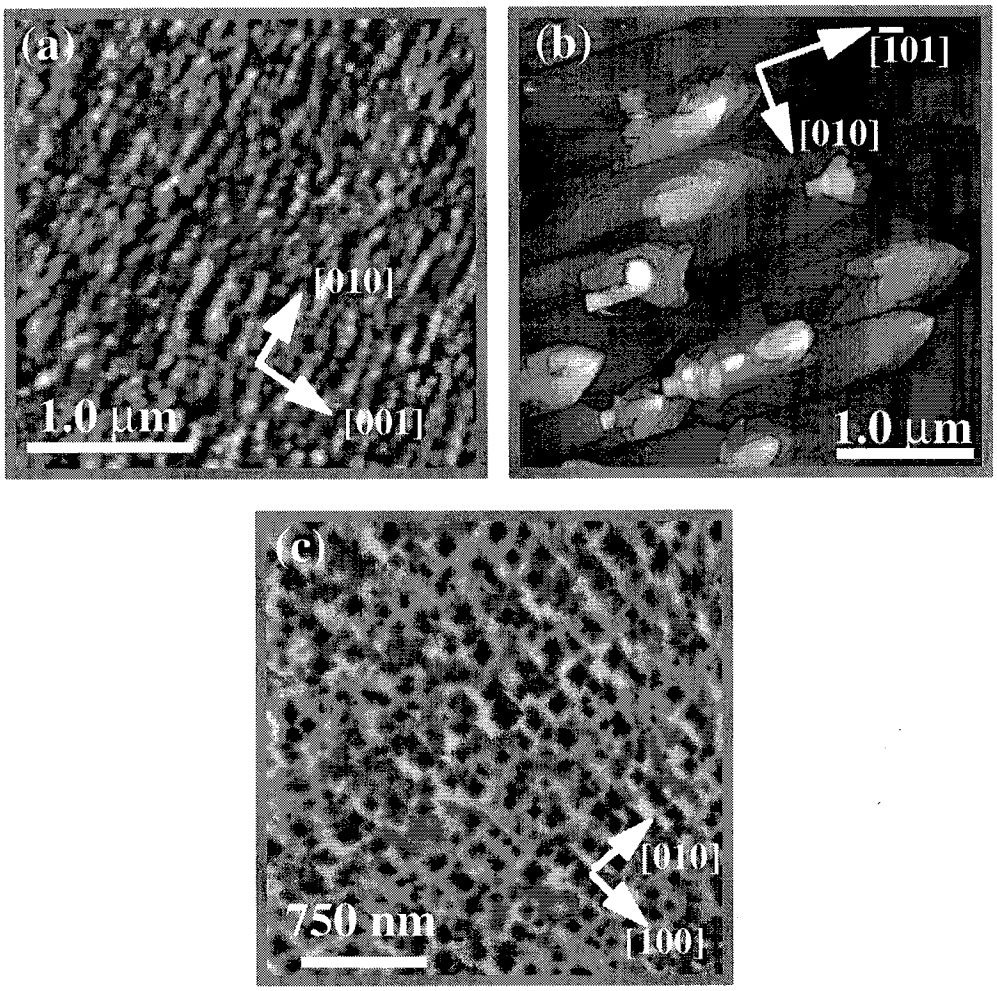

Figure 4. Topographic AFM images of heteroepitaxial rutile films. In the image of the (100) surface (a), the vertical black-to-white scale is 25 Å. The image of the (101) surface (b) has a vertical scale of 300 Å. The image of the (001) surface (c) has a vertical scale of 400 Å.

Homoepitaxial films with the same orientations exhibited island morphologies (See Fig. 3). For example, the islands that make up the (100) film are about 100 nm wide along [010] and about 4 times as long along [001]. The vertical height differences are about 30 to 50 Å. While the size and aspect ratio of the islands are accurately measured, their ill-defined rounded shapes are probably

an artifact caused by the finite size of the probe. The islands on the (101) film are comparable in size, but they have flat tops which allows higher resolution images to be recorded. In this case, the islands are approximately equiaxed and curved steps are apparent. The (001) surface shows a very fine scale island structure; considering the apparent size, the shapes of these islands are more representative of the probe tip than of the crystal surface. Even though the image does not reveal the true size and shape of the features, we can be confident that the surface has a nonplanar, granular structure with features that are less than or equal to the diameter of the tip (typically 100 nm).

Topographic images of the heteroepitaxial films are shown in Fig. 4. The (100) film has fine-scale island features oriented along the [001] direction. The orientation of the islands is the same as in the homoepitaxial layers, but their lateral size is much smaller. The islands found on the (101) heteroepitaxial films are much larger and less isotropic than those observed on the surface of the homoepitaxial layer. Typical islands are about 1 μm long in the $[\bar{1}01]$ direction, 100 to 500 nm wide in the [010] direction, and have flat, stepped plateau tops. The morphology of the (001) heteroepitaxial film is characterized by square, faceted pits (the dark areas of the image). The edges of the square pits are oriented along the [010] and [100] directions.

DISCUSSION

The terraced morphology of the single crystal (100) and (101) surfaces reflects the relative stability of these facets with respect to the (001) surface (see Figs. 1 and 2). Although little is known about rutile's surface energies and equilibrium shape, mineralogists have observed that natural specimens are usually bounded by {110}, {011}, and {100} facets [3]. Based on ultrahigh vacuum (UHV) annealing studies, the (001) surface is believed to be unstable. Different authors have observed that it facets to {011}, {114}, and {111} orientations, depending on the treatment [4,5]. Furthermore, recent first principles pseudopotential calculations have concluded that the {110}, {011}, and {100} facets have relatively low energies with respect to {001} [6]. The results of the

calculations, summarized in Table I, show that the surface energies increase as the Ti cation decreases from its ideal value of 6.

Table I. Rutile surface energies based on data in ref. [6]

orientation	energy (J/m^2)	average Ti coord.
(110)	0.89	5.5
(100)	1.12	5
(011)	1.40	5
(001)	1.66	4

Because UHV annealing is always accompanied by a certain degree of reduction, it is not clear that the same faceting process should occur in oxidizing conditions (air) where the crystal stoichiometry is more nearly ideal. However, this instability might explain the fine scale contrast in Fig. 2. Assuming that the (001) plane decomposes to form {011} facets, the lines of contrast along [010] can be formed by the intersection of complementary (101) and $(\bar{1}01)$ planes and the contrast along [010] can be formed by the intersection of complementary (011) and $(0\bar{1}1)$ planes. An alternate possible arrangement is that the four {101}-related facets meet in a pyramidal structure; this is the observed morphology of the heteroepitaxial films of the same orientation. Although further experiments will be required to understand the origin of the domain structure and the nature of the fine scale facets, it seems likely that it is related to the instability of the (001) surface.

The differences in the morphology of the single crystal films and the homoepitaxial layers is striking; instead of a terraced or faceted structure, we see an island-like morphology that is characteristic of films produced by three dimensional growth [1,2]. The origin of these islands is puzzling since there should be no strain at the substrate/film interface. A plausible explanation for this phenomenon is that impurities at the surface created unanticipated interfacial strains. Chemical analysis by inductively coupled plasma spectroscopy indicated that the crystals contained a relatively high concentration of impurities, which totaled 1.8 % (mole impurity/mole rutile). The primary impurities were K and S. The balance was made up by small concentrations of Al, Ca, Si, and Fe. These concentrations are likely to be enhanced at the surface by segregation and might lead to heterogeneous nucleation of the relatively more pure film.

After nucleation of the islands, three dimensional growth can be sustained by growth rate anisotropies. In other words, if the planes bounding the islands parallel to the substrate advance at a greater velocity than the orientations perpendicular to the substrate plane, the collection of nuclei on the substrate surface leads to the columnar microstructure. If we assume that crystal planes advance at a rate inversely proportional to their surface energy, then the data in Table I indicates that the surfaces studied can always be bounded by lower energy, lateral facets. It is interesting to note that the island size increases as the surface energy of the normal facet (and presumably the growth rate anisotropy) decreases. It would, therefore, be enlightening to examine (110) homoepitaxial films because this orientation is believed to have the lowest surface energy.

The morphologies of the heteroepitaxial films illustrate the combined effects of anisotropic surface energies, growth rates, and interfacial strains. Table II summarizes the relative orientations of the in-plane and normal vectors. Comparing the homoepitaxial and heteroepitaxial film morphologies illustrates the importance of lattice mismatch strain. Note that both the homoepitaxial (100) and heteroepitaxial (100) films have islands elongated along the [001] direction. However, the islands in the heteroepitaxial film are much smaller. Based on this comparison, we conclude that the island size is not limited by the anisotropy of growth rates, but by the mismatch strain.

Table II. Summary of TiO_2 epitaxial film orientations

Film//Substrate Orientation	In-plane alignment and lattice mismatch in that direction (R = TiO_2, C = Al_2O_3)
(100) TiO_2//(0001) Al_2O_3	$[001]_R$//$[01\bar{1}0]_C$ 7.3%; $[010]_R$//$[\bar{2}110]_C$ 3.8%;
(101) TiO_2//(11$\bar{2}$0) Al_2O_3	$[\bar{1}01]_R$//$[\bar{1}100]_C$ 0.9%; $[010]_R$//$[0001]_C$ 5.8%;
(001) TiO_2//(10$\bar{1}$0) Al_2O_3	$[100]_R$//$[11\bar{2}0]_C$ 3.6%; $[010]_R$//$[0001]_C$ 5.2%;

The effect of different mismatch strains can also be seen in the (101) films. While the homoepitaxial layer has a roughly equiaxed structure, the islands in the heteroepitaxial film are elongated along the $[\bar{1}01]$ direction, where the mismatch is smallest. This does not, however, explain why the islands are larger and more faceted. Note that in the heteroepitaxial layer, each island is distinctly bounded on

its lateral edges by (111) planes and in the $[\bar{1}01]$ direction, the islands terminate in a point where the {101} facets meet. On the other hand, the steps on the surface of the homoepitaxial layer can assume all orientations with equal probability. The relation of the island shape to the bulk crystal form is illustrated in Fig. 5. The island size in films that grow by a three dimensional mechanism is known to depend on the growth temperature, the growth rate, film thickness, and the planar density of surface defects [2,7,8]. In this case, the film thickness, growth temperature, and growth rate were held as constants, so we assume that surface quality plays a role. We anticipate that a future examination of as-received substrates might resolve this issue.

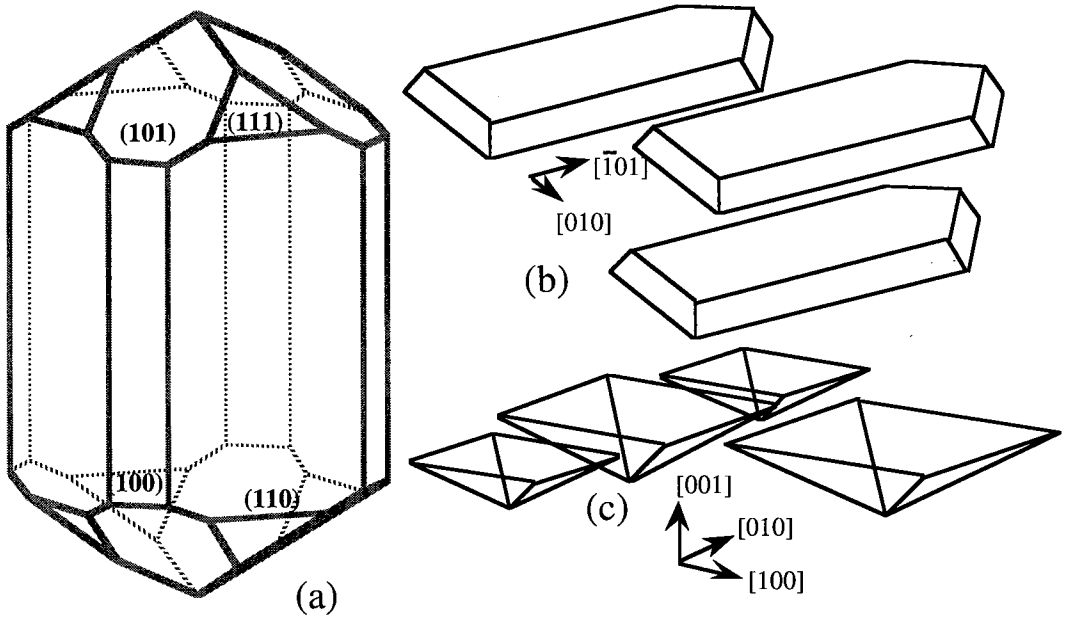

Figure 5. (a) a model for the bulk crystal, showing the relative orientation of low energy faces. An illustration of the island shapes found on (101) oriented films (b) and (001) oriented films.

Like the (101) films, the (001) heteroepitaxial film has more clearly defined facets and a larger island size than the homoepitaxial film. In this case, four {101} facets meet to form an inverted pyramid (see the model in Fig. 5). The inverted shape arises because of the inverse relation between the surface energies and the

growth rates; the lines where the facets meet are nearly parallel to the high energy (001) orientation and, therefore, grow beyond the lower energy {101} faces.

CONCLUSIONS

In this paper, we have described the surface morphologies of the (100), (101), and (001) surfaces of rutile single crystals, homoepitaxial layers, and heteroepitaxial layers. While the single crystal surfaces have flat terraced morphologies, the thin films all have an island structure that results from three dimensional growth. Because the film thickness, growth rate, and growth temperature were held constant in this study, the morphology differences are attributed to the anisotropy of rutile's surface energy and the purity and structure of the substrate surface.

ACKNOWLEDGMENTS

Portions of this material are based on work supported under a National Science Foundation Graduate Fellowship. G.S.R acknowledges support from the National Science Foundation under a YIA grant DMR-9458005 and J.G. was supported by an REU supplement to that grant.

REFERENCES

[1] P.A. Morris-Hotsenpiller, G.A. Wilson, A. Roshko, J.B. Rothman, G.S. Rohrer, "Heteroepitaxial Growth of TiO_2 films by Ion-Beam Sputter Deposition", J. Cryst. Growth, **166** 779-785 (1996).

[2] P.A. Morris-Hotsenpiller, A. Roshko, J.B. Lowekamp, G.S. Rohrer, "Growth Morphologies of Heteroepitaxial Rutile Films on Sapphire Substrates", J. Cryst. Growth, **174** 424-33 (1997).

[3] V. Henrich and P. Cox, "The Surface Science of Metal Oxides", Cambridge University Press, Cambridge, 1994.

[4] L. Firment, "Thermal Faceting of the Rutile TiO_2(001) Surface", Surf. Sci. **116** 205-16 (1982).

[5] G.E. Poirier, B.K. Hance, J.M. White, "Identification of the Facet Planes of Phase I TiO_2(001) rutile by Scanning Tunneling Microscopy and Electron Diffraction", J. Vac. Sci. Technol. B**10** 6-15 (1992).

[6] M. Ramamoorthy, D. Vanderbilt, R.D. King-Smith, "First Principles Calculations of the Energetics of Stoichiometric TiO_2 Surfaces" Phys. Rev. B **49** 16721-27 (1994).

[7] G. B. Stringfellow, "Organic-Metallic Vapor-Phase Epitaxy: Theory and Practice", Academic Press, Inc., San Diego, 1989.

[8] A. Roshko, F. J. B. Stork, D. A. Rudman, D. J. Aldrich, P. A. Morris Hotsenpiller, "Comparison of Heteroepitaxial $YBa_2Cu_3O_{7-\delta}$ and TiO_2 Thin Film Growth", J. Cryst. Growth **174** (1997) 398-408.